

1 **Investigating Elastic Relaxation Effects on the Optical Properties of Functionalised**
2 **Calcium Carbonate Compacts using Optics-Based Heckel Analysis**

3 Prince Bawuah^{a*}, Anssi-Pekka Karttunen^a, Daniel Markl^b, Cathy Ridgway^c, Ossi Korhonen^a,
4 Patrick Gane^{c,d}, J. Axel Zeitler^e, Jarkko Ketolainen^a, Kai-Erik Peiponen^f

5 ^aSchool of Pharmacy, Promis Centre, University of Eastern Finland, P.O. Box 1617, FI-
6 70211, Kuopio, Finland

7 ^bStrathclyde Institute of Pharmacy and Biomedical Sciences, University of Strathclyde, 161
8 Cathedral Street, G4 0RE Glasgow, UK

9 ^cOmya International AG, CH-4665 Oftringen, Switzerland

10 ^dAalto University, Chemical Engineering, Bioproducts and Biosystems, FI-00076 Aalto,
11 Helsinki, Finland

12 ^eDepartment of Chemical Engineering and Biotechnology, University of Cambridge, Philippa
13 Fawcett Drive, CB3 0AS Cambridge, United Kingdom

14 ^fInstitute of Photonics, University of Eastern Finland, P.O. Box 111, FI-80101 Joensuu,
15 Finland

16
17 **Corresponding author:** Prince Bawuah

18 Electronic address: prince.bawuah@uef.fi

19 Phone: +358504120591

20 Address: School of Pharmacy, Promis Centre, University of Eastern Finland, P.O. Box 1617,
21 FI-70211, Kuopio, Finland

29 **Abstract**

30 Heckel analysis is a widely used method for the characterisation of the compression behaviour
31 of pharmaceutical samples during the preparation of solid dosage formulations. The present
32 study introduces an optical version of the Heckel equation that is based on combination of the
33 conventional Heckel equation together with the linear relationship defined between the
34 effective terahertz (THz) refractive index and the porosity of pharmaceutical tablets. The
35 proposed optical Heckel equation allows us to firstly, calculate the zero-porosity refractive
36 index, and secondly, predict the in-die development of the effective refractive index as a
37 function of the compressive pressure during tablet compression. This was demonstrated for
38 five batches of highly porous functionalised calcium carbonate (FCC) excipient compacts. The
39 close match observed between the estimated in-die effective refractive index and the
40 measured/out-of-die effective THz refractive index confirms the validity of the proposed form
41 of the equation. By comparing the measured and estimated in-die tablet properties, a clear
42 change in the porosity and hence, the effective refractive index, due to after-compression elastic
43 relaxation of the FCC compacts, has been observed. We have, therefore, proposed a THz-based
44 compaction setup that will permit in-line monitoring of processes during tablet compression.
45 We envisage that this new approach in tracking powder properties introduced in this
46 preliminary study will lead to the onset of further extensive and detailed future studies.

47 **Keywords:** Heckel law; pharmaceutical tablet; elastic relaxation; porosity; terahertz refractive
48 index

49 **1. Introduction**

50 The numerous advantages that come with the use of pharmaceutical tablets have led to
51 significant investments by the pharmaceutical industry into the study of powder compaction as
52 well as controlling the quality of the finished products. Typical pharmaceutical tablets are
53 composed of several excipient and active pharmaceutical ingredient (API) particles that
54 undergo a vast complexity of processes during compression. The initially loose powder bed
55 undergoes dramatic changes as a function of the relative density due to the force of compaction
56 applied by the tablet punch. These changes include particle rearrangements, elastic and plastic
57 deformation as well as brittle fracture of particles depending on their mechanical properties.
58 Moreover, porosity, distribution of internal stress and density (Kawakita and Lüdde, 1971;
59 Ryshkewitch, 1953) as well as the crystal habit of a drug (Rasenack and Müller, 2002) affect
60 the tableting behavior and the quality properties of the finished tablet.

61 Despite sustained research into powder compaction there are still open questions regarding the
62 complex nature of tableting processes. It is still challenging to successfully predict the
63 properties of the end-tablet product even when all the compositions of the powder mixture are
64 exactly known. Over the past decades a number of experimental techniques and a wide variety
65 of compaction models (Çelik, 1992; Çelik and Marshall, 1989; Krycer et al., 1982; Paronen,
66 1986; Salleh et al., 2015; Sun and Grant, 2001) have been developed and utilised to characterise
67 compression behaviour, i.e. compressibility, compactibility, and pressure susceptibility of
68 pharmaceutical powders. These models are mostly empirical and define criteria to guide the
69 rational selection of suitable excipients to meet the desired properties of the dosage form.
70 However, many of these models are valid within a restricted range of compaction force and
71 can only describe the compaction process of specific pharmaceutical materials (Çelik, 1992;
72 Kolařík, 1994; Van Veen et al., 2004; Wu et al., 2005).

73 The most widespread models are described in terms of the Heckel equation (Heckel, 1961a,
74 1961b), the Kawakita equation (Lüdde and Kawakita, 1966), the Drucker-Prager-Cap model
75 (Han et al., 2008), the modified Heckel equation by Kuentz and Leuenberger (Kuentz and
76 Leuenberger, 1999) and the approach according to Cooper and Eaton (Cooper and Eaton,
77 1962). The Heckel model, which is by far the most popular in the field of powder compression,
78 is of special interest for the present study. Although several authors have highlighted a number
79 of limitations (Rue and REES, 1978) and have proposed modified versions of the Heckel model
80 (Stirnemann et al., 2014), its chief merit is its simplicity together with the readily available
81 reference dataset for different kinds of pharmaceutical materials. This makes the analysis and
82 comparison of different pharmaceutical materials more convenient when the Heckel equation
83 is adopted.

84 Based on the inevitable need for an analytical model during the preparation of solid dosage
85 formulations, the present study considers the Heckel equation but introduces an optical-related
86 version, which is henceforth referred to as “optical Heckel”. The proposed optical Heckel
87 concept originates from the linear correlation observed between the terahertz (THz) based bulk
88 refractive index (effective refractive index) and the bulk porosity of pharmaceutical tablets
89 (Bawuah et al., 2016b; Markl et al., 2018a). With terahertz time-domain spectroscopy (THz-
90 TDS), the effective refractive index, which is a function of the total porosity of a given tablet,
91 can be measured in a nondestructive and contactless fashion within seconds. Based on the
92 unique advantages associated with optical/THz based measurement techniques, we believe that
93 this new optical Heckel equation can serve as a complementary model for rendering

94 comprehensive insight into the processes and compaction mechanisms of pharmaceutical
95 powders.

96 Pharmaceutical industry is currently under transition from traditional batch manufacture to
97 continuous manufacture (Lee et al., 2015; Nasr et al., 2017). One improvement that is usually
98 coupled with continuous manufacture is continuous process monitoring using Process
99 Analytical Technology (PAT) tools. A key to successful implementation of real-time release
100 (RTR) is the ability to monitor processes continuously based on real-time analysis and control
101 of the manufacturing process. Since the compaction process is one of the key operations in a
102 continuous manufacturing plant, it is particularly important to control the physical and
103 chemical properties of tablets. RTR testing is only possible on the basis of a firm understanding
104 of the process and the relationship between process parameters, material attributes and product
105 attributes (European Medicines Agency, 2012). A robust physical model that is sensitive
106 enough and intuitive to use is a key requirement to design and control tablets with
107 required/specific out-of-die properties. This is possible by utilising observed relations between
108 THz-TDS and important tablet parameters, as we have reported in our previous THz-TDS
109 based experiments (Bawuah et al., 2016a, 2016b, 2014a, 2014b, Chakraborty et al., 2017, 2016,
110 Markl et al., 2017a, 2017b).

111 Here, we verify the validity of the proposed optical Heckel method using a two-phase
112 pharmaceutical compact consisting of air-filled pores and a solid material, in the form of a
113 recently developed excipient, functionalised calcium carbonated (FCC), chosen due its
114 complex porous particle behaviour unlike that of other commonly used solid excipients. This
115 excipient presents a more challenging case study for applying conventional modelling
116 approaches.

117 The present study also investigates the existence of elastic relaxation of the FCC compacts after
118 compression based on their in-die and out-of-die porosity as well as height values. To further
119 ascertain the influence of the elastic relaxation on the optical properties of tablets during and
120 after compression, this study estimates the in-die effective refractive index based on the
121 proposed optical Heckel method and compares to the measured counterpart. Elastic relaxation
122 during (Anuar and Briscoe, 2009) and after (Baily and York, 1976) ejection has major influence
123 on, especially, the mechanical and microstructural properties of the finished tablets. We believe
124 that by successfully introducing these optical methods through a carefully engineered

125 compaction setup, it is possible to realise in-line quality control of each tablet during and after
126 compression.

127 2. Theory

128 The conventional Heckel equation (Heckel, 1961a, 1961b) describes the relationship between
129 the logarithmic inverse of the porosity, $f = 1 - \delta$ with δ as the relative density, and the applied
130 compressive pressure, p . The Heckel equation was derived based on the assumption that the
131 in-die densification of the bulk powder obeys first order kinetics as,

$$132 \ln\left(\frac{1}{f}\right) = -\ln f = Kp + A \quad (1)$$

133 where K is a constant of proportionality describing the development of a log-linear response of
134 the structure to the application of pressure, i.e. the Heckel slope, and A is an intercept constant
135 describing densification by particle movement and rearrangement. The inverse of K is the mean
136 yield pressure and it represents the limit of plastic deformation of materials or the resistance of
137 a material to deformation (Hersey and Rees, 1971).

138 The measurement of the refractive index of tablets via THz-TDS has been studied extensively
139 using both the frequency-domain (Bawuah et al., 2016b; Markl et al., 2017b) and time-domain
140 analytical approaches (Bawuah et al., 2016b, 2014a; Markl et al., 2017b). The bulk THz
141 refractive index measured for a given tablet is also referred to as the effective refractive index
142 (n_{eff}) due to the multicomponent nature of a typical pharmaceutical tablet (Bawuah et al.,
143 2014a). Based on empirical evidence, a linear correlation between the effective refractive index
144 and the porosity of pharmaceutical tablets composed of different materials and covering a wide
145 range of porosities was observed (Markl et al., 2018a).

$$146 n_{\text{eff}}(f) = n(0) + (1 - n(0))f \quad (2)$$

147 where $n(0)$ represents the zero-porosity refractive index, i.e. the inherent refractive index of the
148 the solid material constituent in the absence of any imperfections or porosity. During data
149 acquisition, nitrogen gas was used to purge the sample compartment to reduce the effect of
150 water vapor on the terahertz transmission measurement and hence, the unity in Eq. (2)
151 represents the refractive index of air/nitrogen gas ($n_{\text{air}}=1$). Eq. (2) is called the zero-porosity
152 approximation (ZPA) method, which is a complementary method, vis-a-vis effective medium
153 theory (EMT), for the estimation of the porosity from known n_{eff} of a given tablet (Markl et al.,
154 2017b). However, the estimation of porosity of pharmaceutical tablets using Eq. (2) is outside
155 the scope of this study. In the present study, we intend rather to monitor the in-die development

156 of n_{eff} during the compression process using Eq. (2). With a compaction simulator, it is possible
157 to measure the in-die porosity based on in-die densification of the bulk powder, i.e. change in
158 the relative density with respect to increasing compressive force. Equation (2), therefore, serves
159 as the basis for the derivation of the proposed optical counterpart of the Heckel law. From Eqs.
160 (1) and (2) we can solve the following expression for the pressure dependent effective
161 refractive index as follows:

$$162 \quad n_{\text{eff}}(p; f) = n(0) - (n(0) - 1)e^{-(Kp+A)} \quad (3)$$

163 From Eq. (3), we claim that n_{eff} is directly proportional to the result of the Heckel law, and
164 hence it can be used as an alternative or a complementary quantity to $\ln(1/f)$. Moreover, based
165 on the direct use of Eq. (2), i.e. in the derivation of Eq. (3), as well as its applicability for
166 different types of pharmaceutical powders (Markl et al., 2018a), we propose that the optical
167 Heckel model can serve as a complementary general model for characterising the compaction
168 behaviour of different types of pharmaceutical powders. The compression process can be treated
169 as an adiabatic thermodynamic process, where all the thermodynamic variables, such as,
170 volume, pressure and absolute temperature (T) are subject to change. In a study conducted by
171 Wurster and Buckner (Wurster and Buckner, 2012), compaction-induced thermodynamic
172 changes during the compression of anhydrous lactose, a common pharmaceutical excipient,
173 has been characterised.

174 To tackle the mechanisms involved in the compression process of the powder bed rigorously,
175 one should take into consideration the effect of temperature and pressure on the n_{eff} (Wax and
176 Cleek, 1973). However, taking into consideration the temperature dependent n_{eff} will yield a
177 quite challenging situation due to the porous nature of a tablet, which comprises both solid
178 medium and air. In principle, the solid skeleton could be treated by invoking the Mie-Grüneisen
179 model and considering air as an ideal gas similar to dealing with the state equation of highly
180 porous materials with closed and isolated pores (Belkheeva, 2015). Even with this assumption,
181 it is still quite cumbersome to derive the equation of state for pharmaceutical compacts due to
182 their complex nature, i.e. a typical tablet consists of API and various excipient particles as well
183 as both isolated and connected pores. Based on the abovementioned difficulties, this study
184 employs a simple expression as given in Eq. (3) to powder compression. In parallel, we wish
185 to remark that it is possible, in principle, to gain experimental information on both the
186 temperature and pressure dependence of effective refractive index (Wax and Cleek, 1973).
187 Nonetheless, the ZPA refractive index, $n(0)$, used in the calculations of this study is obtained

188 at normal atmospheric pressure and at room temperature. Obviously, for rigorous analysis of
189 the in-die data, the zero porosity refractive index $n(0)$ should be replaced by high pressure and
190 absolute temperature dependent zero porosity refractive index, $n(0, p, T)$, which corresponds
191 to the thermodynamic state of the compact inside the die. However, the thermodynamically
192 dependent refractive indices of the FCC compacts are unknown. Therefore, the present study
193 utilises the estimated zero porosity refractive index, $n(0)$.

194 **3 Materials and Methods**

195 **3.1 Materials**

196 The training set of powder compacts was prepared from FCC (Omyapharm[®]; Omya
197 International AG, Oftringen, Switzerland). The FCC powder is composed of core-shell
198 structured particles in which agglomerated ultrafine calcium carbonate particulates are
199 surrounded by lamellae of hydroxyapatite, thus forming a dual porosity compact. A detailed
200 discussion on the formation of FCC (a highly porous plate-like, nanometre thick lamellar
201 structure of high surface area) has been reported previously (Markl et al., 2017b). A typical
202 pharmaceutical FCC particle consists of a calcium carbonate/hydroxyapatite ratio of 15 % -
203 20 % calcium carbonate to 80 % - 85 % hydroxyapatite.

204 **3.2 Tableting**

205 With a compaction simulator (PuuMan Ltd, Kuopio, Finland), the FCC powder was directly
206 compressed into flant-faced, cylindrical tablets with target height and diameter of 1.5 mm and
207 10 mm, respectively. A range of final compaction levels were achieved by varying the mass of
208 material in the tablet, resulting in tablets that spanned a wide range of porosities. The highly
209 porous nature of the FCC particles permitted the manufacturing of five batches of tablets with
210 increasing porosity starting from a targeted total porosity of 45 % rising to 65 % in 5 %
211 increments (Table 1). Each batch consisted of 15 tablets.

212 During the compaction process, both the upper and lower punch forces as well as upper punch
213 displacement were logged. Figs. 1(a) and (b) show both the compressive force and
214 displacement-time profiles for each batch of tablets. The in-die tablet thickness/height at any
215 compressive pressure (Fig. 1(c)) was tracked as the difference between the lower punch
216 displacement and the upper punch displacement. It is worth mentioning that during the
217 calculation of the punch displacement, deformation of the tooling was taken into consideration.

218 The in-die tablet density was then calculated from the weight and thickness of the tablet at a
219 given compressive pressure. Given the true density of the material in conjunction with the known

220 in-die tablet density, the relative density, and, hence, the in-die porosity, were extracted. We
221 wish to mention that the in-die parameter extraction approach does not take into account the
222 elastic relaxation that occurs after the compaction step. The elastic relaxation causes an
223 increase of the tablet height and porosity, which in turn influences other material parameters
224 extracted from the fitted Heckel plots (Çelik, 1992). In a study conducted by Celik and Marshall
225 (Çelik and Marshall, 1989), it was observed that the differences in the tablet dimensions due to
226 the use of the in-die and out-of-die methods significantly influenced the final Heckel plots.
227 Nonetheless, due to the ease of data collection as well as measurement speed, the in-die
228 approach is still widely used.

229 **3.3 Methods**

230 **Terahertz Time-Domain Spectroscopy (THz-TDS):** Terahertz time-domain measurements
231 were acquired using a Terapulse 4000 spectrometer (Teraview Ltd., Cambridge, UK) in
232 transmission mode. The transmission chamber was purged with dry nitrogen gas throughout
233 the measurement and the noise was reduced by co-averaging 60 measurements. Each time-
234 domain waveform covered a range of 150 ps using a resolution of 0.1 ps, and the total
235 measurement time of the co-averaged waveforms was 1.5 min. The effective refractive index,
236 n_{eff} , of a sample can be calculated from these terahertz measurements either by simply
237 comparing a reference waveform from a known material, e.g. an empty chamber that is purged
238 with dry nitrogen gas ($n_{\text{air}} = 1$), or by considering the fraction of components of known
239 refractive index in the tablet under a range of porosities and extrapolating to zero porosity to
240 provide the reference for scaling. Since the particle size of FCC (12.1 μm) is significantly
241 smaller than the wavelength, $\lambda = 300 \mu\text{m}$, at which we evaluated the refractive index, the
242 effect of scattering is negligible. Therefore, a reduction in particle size during the compaction
243 does not influence the refractive index measurements in terms of scattering. In other words,
244 any dynamic change of sub wavelength particle size is lost.

245 **4 Results and discussion**

246 In this study, both in-die and out-of-die Heckel analysis based on the conventional Heckel
247 equation and the proposed optical Heckel equation have been performed using compression
248 data of FCC compacts.

249 **4.1 Conventional Heckel analysis**

250 For the sake of comparison, we have performed both in-die and out-of-die conventional Heckel
251 plots as shown in Fig. 2. In each case, the compression characteristics of FCC were determined

252 by estimating the slope (K) and the intercept (A) from the Heckel plots (Eq. (1)). The linear
253 portion of the plot was carefully selected to obtain a similar range of compressive pressure
254 for both the in-die and out-of-die data. To meet this condition, only the set B01 was used for
255 the in-die log-linear extrapolation analysis. The slope was obtained by fitting a straight line,
256 whose correlation coefficients (R^2) was not less than 0.99, through data points within the
257 compressive pressure range of around 250 - 370 MPa.

258 Naturally, one would have expected to observe an overlap of the different curves from the in-
259 die Heckel plots for the various batches, since the batches were compressed with the same
260 material (FCC). The shift observed in the Heckel plots means that even though the batches
261 contain the same material, they will have different compression properties, e.g. different slopes
262 and, hence, different yield pressures. The inconsistencies observed emphasise the fact that the
263 conventional Heckel law does not take into consideration the *pressure susceptibility*, which is
264 quite predominant at high relative densities and pressures (Kuentz and Leuenberger, 1999). At
265 low pressures the compression process is dominated by particle rearrangements. In effect,
266 tablets formed at low pressures are essentially particle agglomerates rather than
267 homogeneously dispersed holes in a solid matrix, as rightly stated by Kuentz and Leuenberger
268 (Kuentz and Leuenberger, 1999). Hence, it is not surprising to observe significant differences
269 in the physical behaviour of tablets created at low compressive pressures - in other words
270 tablets with low relative density or high porosity, as demonstrated in the present study (see Fig.
271 2). Kuentz and Leuenberger (Kuentz and Leuenberger, 1999), therefore, introduced a threshold
272 for the porosity or the relative density at which rigidity starts to evolve. That is, a *pressure*
273 *susceptibility* parameter should be taken into consideration for compacts with porosities below
274 the threshold porosity. In this study, the focus was not to adopt the modified Heckel law
275 according to Kuentz and Leuenberger (Kuentz and Leuenberger, 1999), hence, the threshold
276 porosity for the FCC tablets was not estimated. The model in (Kuentz and Leuenberger, 1999)
277 was invoked just to explain the behaviour of the curves in Fig. 2. Nonetheless, such
278 modification can easily be implemented later on if needed.

279 Finally, the differences in values recorded for both K and A in the in-die and out-of-die analyses
280 are due to the relatively low porosities (see Table 2) used in the in-die analysis compared to
281 the relative high porosity values for the out-of-die analysis. The increase in porosity values
282 during the out-of-die analysis is a result of elastic relaxation of the tablets after compression.
283 To buttress our claim of the possible existence of elastic relaxation of the tablets after
284 compression, we tabulate and compare both the in-die and out-of-die tablet thicknesses in Table

285 2. The percentage relative difference, δJ , between the in-die and out-of-die values of the
286 porosity and height/thickness of the tablets is given by

$$287 \quad \delta J = \frac{|J_{\text{out}} - J_{\text{in}}|}{|J_{\text{in}}|} \times 100 \quad (4)$$

288 where J is the tablet parameter, i.e. porosity or height, under consideration, and J_{out} as well as
289 J_{in} are the respective out-of-die and in-die values of the parameter. The results obtained (Table
290 2) indicate relatively high porosity changes, i.e. significant elastic relaxation after compression,
291 for the batch formed under high compressive pressure. Similarly, the relative change in height,
292 as a result of elastic relaxation after compression, is clearly observed for all the batches (Table
293 2).

294 **4.2 Optical Heckel analysis**

295 Similar analysis, as in the case of the conventional Heckel plots (Fig. 2), were performed using
296 the optical Heckel concept as given by Eq. (3). In other words, it is possible to predict, using
297 Eqs. (2) and (3), the development of the effective refractive index during the compressive
298 process of a pharmaceutical compact.

299 Two major analytical steps were taken during the optical Heckel analyses. Firstly, the K and A
300 values, obtained from the in-die conventional Heckel analysis (Fig. 2), were used in addition
301 to the measured THz effective refractive index and the maximum compressive pressure, to
302 calculate the in-die zero-porosity refractive index, $n(0) = n_{\text{in}}(0)$ given in Table 3. The relative
303 change between the estimated $n_{\text{in}}(0)$ with respect to the already known out-of-die zero-porosity
304 refractive index, i.e. $n(0) = n_{\text{out}}(0) = 2.97$ for FCC powder (Markl et al., 2017b), was calculated
305 (Eq. (4)) and tabulated (Table 3). The predicted $n_{\text{in}}(0)$ values, as listed in Table 3, are in a good
306 agreement with the $n_{\text{out}}(0) = 2.97$.

307 Secondly, by using the average value of the $n_{\text{in}}(0)$, i.e. $n_{\text{in}}(0) = 3.088$ with $\delta n(0) = 3.97\%$, in
308 combination with the known values of K , A and the in-die compressive pressure, the in-die
309 effective refractive index, $n_{\text{eff.in}}(p;f)$, defined by Eq. (3), was calculated and compared to the
310 out-of-die effective refractive index, $n_{\text{eff.out}}$ (see Fig. 3). Also, the in-die effective refractive
311 index at maximum compressive pressure, $n_{\text{eff.in}}(p_{\text{max}})$, is compared to the measured (out-of-die)
312 THz effective refractive index, $n_{\text{eff.out}}$ (Table 3). The black dots in Fig. 3 indicate the $n_{\text{eff.in}}$.

313 A close match is observed between the in-die and the out-of-die effective refractive index as
314 shown in Fig. 3 where the calculated in-die effective refractive index data nicely fits the data
315 of the out-of-die effective refractive index. The calculated low relative change, δn_{eff} , of the

316 effective refractive index (Table 3) also attests to the observed close match between the in-die
317 and the out-of-die effective refractive index, which proves the accuracy of the estimated ZPA
318 $n(0)$ using this newly proposed optical Heckel method. In other words, the proposed optical
319 Heckel method can serve as a complementary method to the ZPA method for accurate
320 prediction of the zero-porosity refractive index of tablets. However, the relative low differences
321 observed between the values of the calculated in-die effective refractive index, $n_{\text{eff.in}}$, and the
322 measured/out-of-die effective refractive index ($n_{\text{eff.out}}$), might be attributed to the presents of
323 elastic relaxation of the tablets after compression. Additionally, the use of the simple ZPA $n(0)$
324 in the calculations without taking into consideration the effect of the relatively high in-die
325 temperature and pressure during compression, as already mentioned in section 2, can be a
326 contributing factor to the observed relative change in the effective and intrinsic refractive
327 indices. Finally, differences in the moisture content of the samples, as well as experimental
328 errors during the in-die and out-of-die measurements, can significantly contribute to the
329 observed discrepancies in the refractive indices.

330 The above promising experimental observation in addition to the zero offset in the optical
331 Heckel plots (Fig. 3) suggest the validity of the linear relation between n_{eff} and f as defined in
332 Eq. (2) and utilised in Eq. (3). In other words, the purely experimental data gives support to the
333 theoretical models given in Eqs. (2) and (3). The effective refractive index is a basic optical
334 property that can be measured easily by terahertz time-domain technology (Bawuah et al.,
335 2016a, 2016b, 2014a, 2014b, Chakraborty et al., 2017, 2016, Markl et al., 2017a, 2017b). This
336 makes terahertz spectroscopy a promising PAT tool for in-line applications in the
337 pharmaceutical industry.

338 Fig. 4 summarises and compares all the estimated relative changes, i.e. porosity, height,
339 effective refractive index, and intrinsic refractive index, that might be caused by the after-
340 compression elastic relaxation of the FCC compacts. There is clearly a change in the porosity
341 as well as effective refractive index due to elastic relaxation. However, the observed relative
342 change in the porosity is not directly correlated to that of the effective refractive index, which
343 buttresses our previous speculation that, aside porosity; thermodynamic parameters, e.g.
344 temperature, have significant influence on the effective refractive index of pharmaceutical
345 tablets, especially during compression. Similarly, the change in the porosity is not directly
346 correlated to the tablet thickness change (Fig. 4). The change in the effective refractive index
347 and porosity clearly indicates the influence of elastic relaxation on the pore structure. This will
348 in turn impact the liquid uptake rate that is part of the disintegration process of pharmaceutical

349 tablets (Markl et al., 2018b). This post-compaction variation of the pore structure will also
350 directly affect the dissolution performance. It is thus of great importance to understand the
351 elastic relaxation effect in the light of quality control – dissolution studies may yield different
352 results when conducted right after compaction compared to them performed several days or
353 weeks after manufacturing. Moreover, the elastic relaxation is a critical mechanism in
354 continuous manufacturing as the change in tablet volume may cause cracks in the subsequently
355 applied coating, which may render the coating function, e.g. improving the appearance,
356 masking an odour, modifying the release characteristics, useless.

357 The close match between the values of the calculated and measured refractive index is an
358 indication of the possibility to conduct optical Heckel analysis using THz technology. By
359 engineering a compaction setup coupled with terahertz pulse imaging (TPI), it would be
360 possible, in principle, to measure the in-die refractive index at a given compressive force as
361 illustrated in the schematic diagram shown in Fig. 5. With the known in-die refractive index,
362 we can extract the values of K and A from a $\ln(n_{\text{eff}}(p;f))$ versus compressive pressure plots (Eq.
363 (3)). One advantage of the proposed optical Heckel analysis over the conventional Heckel
364 analysis is the use of a basic optical property, i.e. refractive index that can be measured directly
365 by THz means. At present, there are no good techniques available to measure porosity in-die
366 (except maybe the use of in situ ultrasound approach), hence, the porosity used in the
367 conventional Heckel plots is mostly calculated from the bulk and true densities of a given
368 powder material. However, accurate measurements of the true density of pharmaceutical
369 powder, especially hydrates, by using helium pycnometry, has raised major concern (Sun,
370 2004). It is important to mention that, currently, the use of the THz-TDS in the detection of the
371 effective refractive index of pharmaceutical tablets is limited to out-of-die method only.
372 Nevertheless, the relatively good match between the calculated (in-die) and measured (out-of-
373 die) refractive index data shows the power of the proposed optical Heckel law to estimate K
374 and A accurately from a non-contact measurement of THz pulse under standard condition
375 (atmospheric pressure). Finally, aside from confirming the validity of the linear relation (Eq.
376 (2)), the close similarity of the calculated ($n_{\text{eff.in}}$) and measured ($n_{\text{eff.out}}$) data also means that
377 both in-die and out-of-die porosity of tablets can now be estimated from their THz refractive
378 index data without using the current not ideal true density approach.

379 **5. Conclusions**

380 This study has successfully introduced and practically demonstrated the newly proposed optical
381 Heckel concepts for fast, non-invasive and accurate characterisation of the compression

382 behaviour of FCC compacts. As a case study, five batches of compressed FCC compacts with
383 different porosity levels were used in the study. The proposed optical Heckel equation was
384 derived based on modified mathematical models formulated as a result of our previous THz-
385 TDS experiments. Close correlations were observed between the in-die and out-of-die optical
386 Heckel analyses without any significant offsets. The close match between the values of the
387 predicted effective THz refractive index, i.e. based on the optical Heckel equation, and the
388 measured THz refractive index of the FCC compacts has shown the feasibility of replacing the
389 porosity with the effective THz refractive index during Heckel analysis. We will work on
390 extending the optical Heckel concept to other popular models such as Leuenberger, and
391 Kawakita using different pharmaceutical materials and biconvex tablets.

392 The present study has also investigated the existence of elastic relaxation of FCC compacts
393 after compression based on the differences observed in both their in-die and out-of-die porosity
394 as well as height values. Furthermore, the study has highlighted the effect of after-compression
395 elastic relaxation on the optical properties, i.e. effective refractive index, of FCC compacts
396 using the newly proposed optical Heckel method. Based on a comparison between the
397 calculated in-die effective refractive index and the measured out-of-die effective refractive
398 index, a clear change in the effective refractive index of the FCC compacts has been observed.
399 The relative change in the effective refractive index is attributed partly to elastic relaxation and
400 partly to thermodynamic effects as well as possible experimental errors.

401 Finally, the proposed optical Heckel method can serve as a complementary method to the ZPA
402 method for accurate prediction of the zero-porosity refractive index of pharmaceutical tablets.
403 Hence, as an initiator of future study, the present work proposes a compaction setup that will
404 allow in-line process monitoring using THz technology.

405 **References**

- 406 Anuar, M.S., Briscoe, B.J., 2009. The elastic relaxation of starch tablets during ejection.
407 Powder Technol. 195, 96–104. <https://doi.org/10.1016/j.powtec.2009.05.019>
- 408 Baily, E.D., York, P., 1976. An apparatus for the study of strain recovery in compacts. J.
409 Mater. Sci. 11, 1470–1474. <https://doi.org/10.1007/BF00540880>
- 410 Bawuah, P., Chakraborty, M., Ervasti, T., Zeitler, J.A., Ketolainen, J., Gane, P.A.C.,
411 Peiponen, K.-E., 2016a. A structure parameter for porous media obtained with the aid of
412 Wiener bounds for effective permittivity and terahertz time-delay measurement. Int. J.
413 Pharm. 506, 87–92. <https://doi.org/10.1016/j.ijpharm.2016.04.026>

414 Bawuah, P., Pierotic Mendia, A., Silfsten, P., Pääkkönen, P., Ervasti, T., Ketolainen, J.,
415 Zeitler, J.A., Peiponen, K.-E., 2014a. Detection of porosity of pharmaceutical compacts
416 by terahertz radiation transmission and light reflection measurement techniques. *Int. J.*
417 *Pharm.* 465, 70–76. <https://doi.org/10.1016/j.ijpharm.2014.02.011>

418 Bawuah, P., Silfsten, P., Ervasti, T., Ketolainen, J., Zeitler, J.A., Peiponen, K.-E., 2014b.
419 Non-contact weight measurement of flat-faced pharmaceutical tablets using terahertz
420 transmission pulse delay measurements. *Int. J. Pharm.* 476, 16–22.
421 <https://doi.org/10.1016/j.ijpharm.2014.09.027>

422 Bawuah, P., Tan, N., Tweneboah, S.N.A., Ervasti, T., Axel Zeitler, J., Ketolainen, J.,
423 Peiponen, K.-E., 2016b. Terahertz study on porosity and mass fraction of active
424 pharmaceutical ingredient of pharmaceutical tablets. *Eur. J. Pharm. Biopharm.* 105,
425 122–133. <https://doi.org/10.1016/j.ejpb.2016.06.007>

426 Belkheeva, R.K., 2015. Equation of state for a highly porous material. *High Temp.* 53, 348–
427 357. <https://doi.org/10.1134/S0018151X15020054>

428 Çelik, M., 1992. Overview of Compaction Data Analysis Techniques. *Drug Dev. Ind. Pharm.*
429 18, 767–810. <https://doi.org/10.3109/03639049209058560>

430 Çelik, M., Marshall, K., 1989. Use of a Compaction Simulator System in Tableting
431 Research. *Drug Dev. Ind. Pharm.* 15, 759–800.
432 <https://doi.org/10.3109/03639048909058530>

433 Chakraborty, M., Bawuah, P., Tan, N., Ervasti, T., Pääkkönen, P., Zeitler, J.A., Ketolainen,
434 J., Peiponen, K.-E., 2016. On the correlation of effective terahertz refractive index and
435 average surface roughness of pharmaceutical tablets. *J. Infrared, Millimeter, Terahertz*
436 *Waves* 37, 776–785. <https://doi.org/10.1007/s10762-016-0262-0>

437 Chakraborty, M., Ridgway, C., Bawuah, P., Markl, D., Gane, P.A.C., Ketolainen, J., Zeitler,
438 J.A., Peiponen, K.-E., 2017. Optics-based compressibility parameter for pharmaceutical
439 tablets obtained with the aid of the terahertz refractive index. *Int. J. Pharm.* 525, 85–91.
440 <https://doi.org/10.1016/j.ijpharm.2017.03.093>

441 Cooper, A.R., Eaton, L.E., 1962. Compaction Behavior of Several Ceramic Powders. *J. Am.*
442 *Ceram. Soc.* 45, 97–101. <https://doi.org/10.1111/j.1151-2916.1962.tb11092.x>

443 European Medicines Agency, 2012. Guideline on Real Time Release Testing.

444 Han, L.H., Elliott, J.A., Bentham, A.C., Mills, A., Amidon, G.E., Hancock, B.C., 2008. A
445 modified Drucker-Prager Cap model for die compaction simulation of pharmaceutical
446 powders. *Int. J. Solids Struct.* 45, 3088–3106.
447 <https://doi.org/doi:10.1016/j.ijsolstr.2008.01.024>

448 Heckel, R.W., 1961a. Density-Pressure Relationships in Powder Compaction. *Trans. Metall.*
449 *Soc. AIME* 221, 671–675.

450 Heckel, R.W., 1961b. An Analysis of Powder Compaction Phenomena. *Trans. Metall. Soc.*
451 *AIME* 221, 1001–1008.

452 Hersey, J., Rees, J., 1971. Particles-deformation of particles during briquetting. *Nature* 230,
453 96. <https://doi.org/10.1038/physci230096a0>

454 Kawakita, K., Lüdde, K.-H., 1971. Some considerations on powder compression equations.
455 *Powder Technol.* 4, 61–68. [https://doi.org/https://doi.org/10.1016/0032-5910\(71\)80001-](https://doi.org/https://doi.org/10.1016/0032-5910(71)80001-3)
456 3

457 Kolařík, J., 1994. A model for the yield strength of binary blends of thermoplastics. *Polymer*
458 *(Guildf)*. 35, 3631–3637. [https://doi.org/10.1016/0032-3861\(94\)90539-8](https://doi.org/10.1016/0032-3861(94)90539-8)

459 Krycer, I., Pope, D.G., Hersey, J.A., 1982. The Interpretation of Powder Compaction Data - a
460 Critical Review. *Drug Dev. Ind. Pharm.* 8, 307–342.
461 <https://doi.org/10.3109/03639048209022103>

462 Kuentz, M., Leuenberger, H., 1999. Pressure susceptibility of polymer tablets as a critical
463 property: A modified Heckel equation. *J. Pharm. Sci.* 88, 174–179.
464 <https://doi.org/10.1021/js980369a>

465 Lee, S.L., O'Connor, T.F., Yang, X., Cruz, C.N., Chatterjee, S., Madurawe, R.D., Moore,
466 C.M.V., Yu, L.X., Woodcock, J., 2015. Modernizing Pharmaceutical Manufacturing:
467 from Batch to Continuous Production. *J. Pharm. Innov.* [https://doi.org/10.1007/s12247-](https://doi.org/10.1007/s12247-015-9215-8)
468 015-9215-8

469 Lüdde, K., Kawakita, K., 1966. Die Pulverkompression. *Pharmazie* 21, 393–403.

470 Markl, D., Bawuah, P., Ridgway, C., van den Ban, S., Goodwin, D.J., Ketolainen, J., Gane,
471 P., Peiponen, K.-E., Zeitler, J.A., 2017a. Fast and Non-destructive Pore Structure
472 Analysis using Terahertz Time-Domain Spectroscopy. *Int. J. Pharm.* 537, 102–110.
473 <https://doi.org/10.1016/j.ijpharm.2017.12.029>

474 Markl, D., Strobel, A., Schlossnikl, R., Bötcher, J., Bawuah, P., Ridgway, C., Rantanen, J.,
475 Rades, T., Gane, P., Peiponen, K.-E., Zeitler, J.A., 2018a. Characterisation of Pore
476 Structures of Pharmaceutical Tablets: A Review. *Int. J. Pharm.* 538, 188–214.
477 <https://doi.org/https://doi.org/10.1016/j.ijpharm.2018.01.017>

478 Markl, D., Wang, P., Ridgway, C., Karttunen, A.-P., Bawuah, P., Ketolainen, J., Gane, P.,
479 Peiponen, K.-E., Zeitler, J.A., 2018b. Resolving the rapid water absorption of porous
480 functionalised calcium carbonate powder compacts by terahertz pulsed imaging. *Chem.*
481 *Eng. Res. Des.* 132, 1082–1090. <https://doi.org/10.1016/j.cherd.2017.12.048>

482 Markl, D., Wang, P., Ridgway, C., Karttunen, A.-P., Chakraborty, M., Bawuah, P.,
483 Pääkkönen, P., Gane, P., Ketolainen, J., Peiponen, K.-E., Zeitler, J.A., 2017b.
484 Characterization of the Pore Structure of Functionalized Calcium Carbonate Tablets by
485 Terahertz Time-Domain Spectroscopy and X-Ray Computed Microtomography. *J.*
486 *Pharm. Sci.* 106, 1586–1595. <https://doi.org/10.1016/j.xphs.2017.02.028>

487 Nasr, M.M., Krumme, M., Matsuda, Y., Trout, B.L., Badman, C., Mascia, S., Cooney, C.L.,
488 Jensen, K.D., Florence, A., Johnston, C., Konstantinov, K., Lee, S.L., 2017. Regulatory
489 Perspectives on Continuous Pharmaceutical Manufacturing: Moving From Theory to
490 Practice: September 26-27, 2016, International Symposium on the Continuous
491 Manufacturing of Pharmaceuticals, in: *Journal of Pharmaceutical Sciences*. Elsevier, pp.
492 3199–3206. <https://doi.org/10.1016/j.xphs.2017.06.015>

493 Paronen, P., 1986. Heckel plots as indicators of elastic properties of pharmaceuticals. *Drug*
494 *Dev. Ind. Pharm.* 12, 1903–1912. <https://doi.org/10.3109/03639048609042616>

495 Rasenack, N., Müller, B.W., 2002. Crystal habit and tableting behavior. *Int. J. Pharm.* 244,
496 45–57. [https://doi.org/10.1016/S0378-5173\(02\)00296-X](https://doi.org/10.1016/S0378-5173(02)00296-X)

497 Rue, P.J., REES, J.E., 1978. Limitations of the Heckel relation for predicting powder
498 compaction mechanisms. *J. Pharm. Pharmacol.* 30, 642–643.
499 <https://doi.org/10.1111/j.2042-7158.1978.tb13347.x>

500 Ryshkewitch, E., 1953. Compression Strength of Porous Sintered Alumina and Zirconia. *J.*
501 *Am. Ceram. Soc.* 36, 65–68. <https://doi.org/10.1111/j.1151-2916.1953.tb12837.x>

502 Salleh, F.S.M., Yusof, Y.A., Anuar, M.S., Chin, N.L., 2015. Understanding the tableting
503 characteristics of *Ficus deltoidea* powder by fitting into compression models. *J. Food*

- 504 Process Eng. 38, 250–261. <https://doi.org/10.1111/jfpe.12165>
- 505 Stirnimann, T., Atria, S., Schoelkopf, J., Gane, P.A.C., Alles, R., Huwyler, J., Puchkov, M.,
506 2014. Compaction of functionalized calcium carbonate, a porous and crystalline
507 microparticulate material with a lamellar surface. *Int. J. Pharm.* 466, 266–275.
508 <https://doi.org/10.1016/j.ijpharm.2014.03.027>
- 509 Sun, C., 2004. A Novel Method for Deriving True Density of Pharmaceutical Solids
510 Including Hydrates and Water-Containing Powders. *J. Pharm. Sci.* 93, 646–653.
511 <https://doi.org/10.1002/jps.10595>
- 512 Sun, C., Grant, D.J.W., 2001. Influence of Elastic Deformation of Particles on Heckel
513 Analysis. *Pharm. Dev. Technol.* 6, 193–200. <https://doi.org/10.1081/PDT-100000738>
- 514 Van Veen, B., Van Der Voort Maarschalk, K., Bolhuis, G.K., Frijlink, H.W., 2004.
515 Predicting mechanical properties of compacts containing two components. *Powder
516 Technol.* 139, 156–164. <https://doi.org/10.1016/j.powtec.2003.11.003>
- 517 Wax, R.M., Cleek, G.W., 1973. The Effect of Temperature and Pressure on the Refractive
518 Index of Some Oxide Glasses. *J. Res. Natl. Bur. Stand. - A. Phys. Chem.* 77A, 755–763.
519 <https://doi.org/10.6028/jres.077A.046>
- 520 Wu, C.Y., Best, S.M., Bentham, A.C., Hancock, B.C., Bonfield, W., 2005. A simple
521 predictive model for the tensile strength of binary tablets. *Eur. J. Pharm. Sci.* 25, 331–
522 336. <https://doi.org/10.1016/j.ejps.2005.03.004>
- 523 Wurster, D.E., Buckner, I.S., 2012. Characterizing compaction-induced thermodynamic
524 changes in a common pharmaceutical excipient. *J. Pharm. Sci.* 101, 2960–2967.
525 <https://doi.org/https://doi.org/10.1016/j.ijpharm.2018.01.017>

526

527 **Table 1**

Tablet batch	m (mg)	H_{out} (mm)	D (mm)	f_{out} (%)
B01	217±2	1.67	10.04	45.50±0.52
B02	190±2	1.64	10.03	50.27±0.50
B03	168±2	1.63	10.02	55.72±0.40

B04	147±2	1.62	10.02	61.02±0.93
B05	122±2	1.61	10.00	67.35±0.79

528 Table 1: A list of the out-of-die properties of the five batches of FCC tablets. The tablet
529 geometry was that of flattop cylindrical, having an axial height, H_{out} , diameter, D , weight, m ,
530 and the calculated nominal porosity, f_{out} , derived from the true density and bulk density. The
531 instruments used for measurement of weight, dimensions as well as the porosity calculation
532 have been described in our previous study (Markl et al., 2017b).

533 **Table 2**

Tablet batch	f_{in} (%)	δf (%)	H_{in} (mm)	δH (%)
B01	44.04	3.32	1.60	4.37
B02	49.95	0.64	1.56	5.13
B03	55.56	0.29	1.57	3.82
B04	60.97	0.08	1.55	4.52
B05	67.36	0.01	1.56	3.21

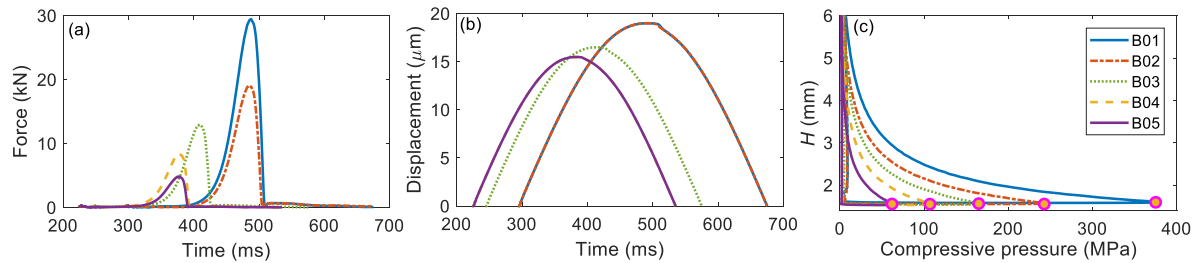
534 Table 2: Estimated in-die values of the average porosity and average height of the five batches
535 of FCC compacts. f_{in} is the in-die porosity values at maximum compressive pressure. δf is the
536 relative change, in percentage, between the out-of-die (see Table 1) and in-die porosity values.
537 H_{in} is the in-die tablet height at maximum compressive pressure. δH is the relative height
538 change, in percentage, between the out-of-die (see Table 1) and in-die data

539 **Table 3**

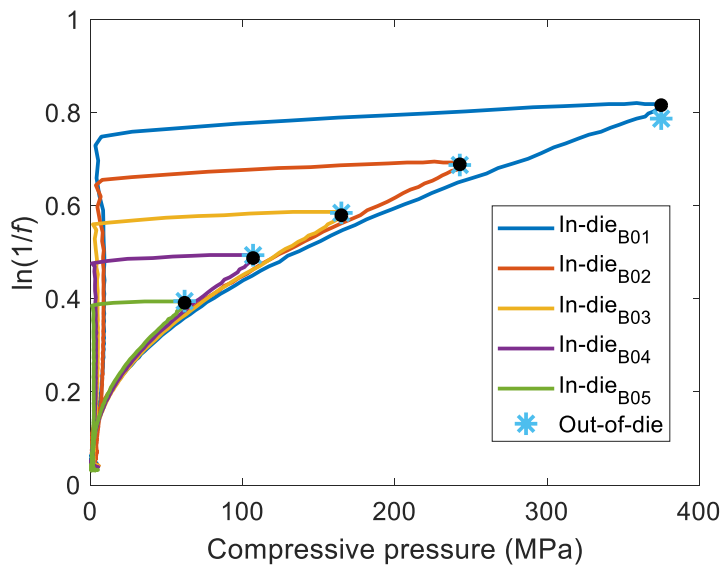
Tablet batch	$n_{\text{eff.out}}$	$n_{\text{eff.in}}$	δn_{eff} (%)	$n_{\text{in}}(0)$	$\delta n(0)$ (%)
B01	2.152	2.172	0.92	3.053	2.79
B02	2.029	2.000	1.45	3.149	6.03
B03	1.916	1.884	1.70	3.164	6.53
B04	1.798	1.789	0.50	3.111	4.75
B05	1.669	1.711	2.45	2.964	0.20

540 Table 3: A comparison between measured THz effective refractive index ($n_{\text{eff.out}}$) and
541 calculated, i.e. using Eq. (3) effective refractive index based on in-die, $n_{\text{eff.in}}$, Heckel analyses.
542 $n_{\text{in}}(0)$ is the calculated zero-porosity refractive index using the in-die K and A values obtained
543 from the conventional Heckel plots (Fig. 2). δn_{eff} is the relative change, in percentage, between
544 the out-of-die and in-die effective refractive index values whereas $\delta n(0)$ is the calculated

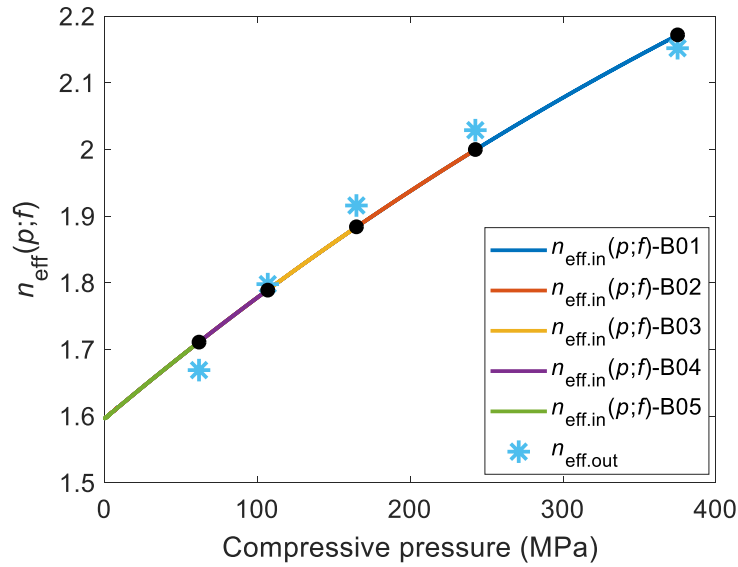
545 relative change in the intrinsic refractive index of FCC using out-of-die, $n_{\text{out}}(0) = 2.97$, and in-
 546 die, $n_{\text{in}}(0)$ refractive indices. Eq. (3), in conjunction with out-of-die effective refractive index
 547 ($n_{\text{eff.out}}$), was used for the calculation of the in-die zero-porosity refractive indices tabulated
 548 below.



549
 550 Fig. 1. Parameters of the compaction of five batches with varying porosity. (a) The compressive
 551 force- and (b) displacement-time profiles for each batch of tablets during compression. (c) In-
 552 die monitoring of the height of the tablets during the compression. The targeted output tablet
 553 height was around 1.5 mm.

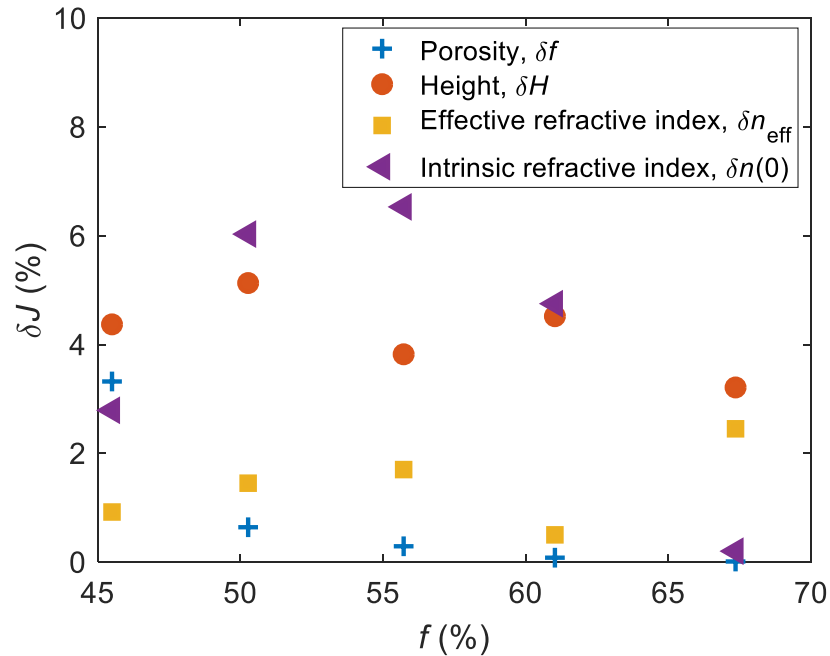


554
 555 Fig. 2. Conventional Heckel plots for the tablet samples using in-die and out-of-die
 556 measurements. From the log-linear extrapolation ($R^2 = 0.99$) using batch B01 for the in-die
 557 analysis, the values of $K = 0.00130 \text{ MPa}^{-1}$ and $A = 0.3361$ were extracted. Out-of-die analysis
 558 of the five batches of FCC tablets using two points for the log-linear extrapolation yielded $K =$
 559 0.00076 MPa^{-1} and $A = 0.5050$. Only batch B01 was used for the in-die analysis due to the
 560 well-defined linear portion between the pressure range of around 250 – 370 MPa, as shown.
 561 This pressure range matches the portion chosen for the log-linear fitting for the out-of-die
 562 analysis. The black dots show the in-die values of $\ln(1/f)$ at the maximum compressive pressure
 563 for each batch.



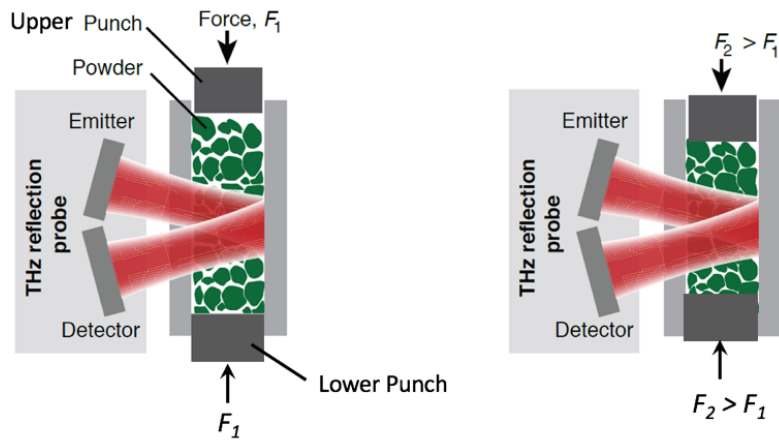
564

565 Fig. 3. Effective refractive index ($n_{\text{eff}}(p;f)$) as a function of the compaction pressure for both
 566 in-die and out-of-die analysis. The parameters $K = 0.00130 \text{ MPa}^{-1}$, $A = 0.3361$, obtained from
 567 the conventional Heckel plots, were used to calculate the $n_{\text{eff.in}}(p;f)$. For the sake of comparison,
 568 we again plot the out-of-die measured THz refractive index, $n_{\text{eff.out}}$, as a function of compressive
 569 pressure. The black dots show the values of $n_{\text{eff.in}}(p;f)$ at the maximum compressive pressure
 570 for each batch.



571

572 Fig. 4. A comparison of the estimated relative change in the porosity, height, effective
 573 refractive index and intrinsic refractive index with respect to the out-of-die porosity.



574

575 Fig. 5. Principle of a proposed future compaction setup coupled with a TPI. (a) Shows the very
 576 beginning of the compression process with the force, F_1 . (b) Indicates an increasing
 577 compressive force, F_2 , which causes an increase of the refractive index. This designed setup
 578 will monitor the dynamic change of the THz refractive index from the beginning to the end of
 579 the compaction process.